# Arbitrary amplitude dust acoustic solitary waves and double layers in nonthermal plasma including the effect of dust temperature

Animesh Das, Anup Bandyopadhyay, and K. P. Das

Citation: Physics of Plasmas (1994-present) **16**, 073703 (2009); doi: 10.1063/1.3170900
View online: http://dx.doi.org/10.1063/1.3170900
View Table of Contents: http://scitation.aip.org/content/aip/journal/pop/16/7?ver=pdfcov
Published by the AIP Publishing

# Arbitrary amplitude dust acoustic solitary waves and double layers in nonthermal plasma including the effect of dust temperature

Animesh Das,[1] Anup Bandyopadhyay,[1] and K. P. Das[2]
[1]*Department of Mathematics, Jadavpur University, Kolkata 700 032, India*
[2]*Department of Applied Mathematics, University of Calcutta, 92 Acharya Prafulla Chandra Road, Kolkata 700 009, India*

(Received 13 March 2009; accepted 16 June 2009; published online 13 July 2009)

A computational scheme has been developed to study the arbitrary amplitude dust acoustic solitary waves and double layers in nonthermal plasma consisting of negatively charged dust grains, nonthermal ions, and isothermal electrons including the effect of dust temperature. The Sagdeev potential approach, which is valid to study the arbitrary amplitude solitary waves and double layers, has been employed. The computation has been carried out over the entire interval of $\beta_1 : 0 \leq \beta_1 < \beta_M$. This $\beta_1$ is a parameter associated with the nonthermal distribution of ions and $\beta_M$ is the upper bound of $\beta_1$. Depending on the nature of existence of solitary waves and double layers, the interval for $\beta_1$ can be broken up into four disjoint subintervals holding the other parameters fixed. By nature of existence of solitary waves and double layers, it is meant that in some subinterval only negative potential solitary waves can exist, whereas in another both negative and positive potential solitary waves can coexist along with a double layer, etc. Corresponding to every $\beta_1$ lying within a subinterval of $\beta_1$, there is a definite interval for the Mach number (definite value of the Mach number) for which there exists solitary waves (double layer) specific for that subinterval of $\beta_1$. The role of dust temperature on the subintervals of $\beta_1$ and on amplitude of solitary waves and double layers has been explored. © *2009 American Institute of Physics*. [DOI: 10.1063/1.3170900]

## I. INTRODUCTION

In recent times interest has grown to the understanding of different types of wave propagation in dusty plasma due to their involvement in the study of astrophysical and space environments, such as cometary tails, asteroid zones, planetary rings, interstellar medium, the earth's environment, etc.[1–9] Rao *et al.*[10] theoretically predicted the existence of extremely low phase velocity dust acoustic (hereafter DA) waves in such plasmas. Actually, they considered an unmagnetized collisionless dusty plasma consisting of Boltzmann distributed electrons and ions and negatively charged dust particles. The existence of the DA waves has been supported by the experimental works of Barkan *et al.*,[11] Praburam and Goree,[12] and Pieper and Goree.[13] Rao *et al.*[10] also considered the DA solitary (hereafter DAS) waves in the same dusty plasma system. In small amplitude limit, where the reductive perturbation method of Washimi and Taniuti[14] is employed, the existence of negative potential DAS wave has been observed. In arbitrary amplitude DAS waves, where the Sagdeev potential technique[15] is used, the existence of negative potential DAS wave has been observed.

To study the linear and nonlinear properties of collisionless plasma, in general, Maxwellian velocity distribution function for each species of particles has been used. However in a number of heliospheric environments the dusty plasma contains nonthermally distributed ions or electrons.[8,9,16–21] For example, nonthermal ions have been observed in and around the Earth's bowshock and foreshock[22,23] and the loss of energetic ions have been observed from the upper ionosphere of Mars.[24] Energetic protons have been observed in the vicinity of the moon.[25] Therefore, it is of considerable importance to study nonlinear wave structures in dusty plasma in which any one or both of the two species (electrons and ions) are nonthermally distributed. Such a study for dusty plasma consisting of nonthermally distributed ions was made by Mamun *et al.*,[18] Mendoza-Briceño and co-workers,[19] and Maharaj *et al.*[20,21] However they demonstrated the possible existence of solitary wave and double layer structures for some sets of values of the parameters of the problem without making any delimination of parameter space for the existence of such nonlinear structures. Recently, Verheest and Pillay[16] and Verheest[17] have given in a systematic way a fluid dynamical description of large amplitude DAS structure in nonthermal plasma showing a clear delimination of the existing domains in their compositional parameter space without including the effect of dust temperature.

Nonthermal distribution of any species of particles (as prescribed by Cairns *et al.*[26] for the electron species) can be regarded as population of Boltzmann distributed particles together with a population of highly energetic particles. This can also be regarded as a modified Boltzmannian distribution, which has the property that the number of particles in phase space in the neighborhood of the point $v=0$ is much smaller than the number of particles in phase space in the neighborhood of the point $v=0$ for the case of Boltzmann distribution, where $v$ is the velocity of the particle in phase space. This type of velocity distribution is often termed as Cairns distribution and was considered by many authors in various studies of different collective processes in plasmas and dusty plasmas.[16–21,27–33]

In the present investigation we reconsider the problem of

 

Verheest and Pillay[16] to include the effect of dust temperature and to elaborate their investigations on delimination of compositional parameter space. A computational scheme has been developed to study arbitrary amplitude DAS waves and double layers in plasma consisting of negatively charged dust grains, nonthermal ions, and isothermal electrons including the effect of dust temperature. The Sagdeev potential approach, which is valid for arbitrary amplitude solitary waves, has been employed. The four basic parameters of the present dusty plasma system are $\mu$, $\alpha$, $\beta_1$, and $\sigma_d$, which are, respectively, the ratio of unperturbed number density of electrons to that of nonthermal ions, the ratio of average temperature of nonthermal ions to that of isothermal electrons, a parameter of the nonthermal distribution of ions, and the ratio of average temperature of dust particles to that of ions divided by the number of negative charges residing on a dust grain surface. It is found that for any fixed values of parameters $\mu$, $\alpha$, and $\sigma_d$ the entire interval of $\beta_1$ can be broken down into four disjoint subintervals: (I) $0 \leq \beta_1 \leq \beta_{1c}$, (II) $\beta_{1c} < \beta_1 \leq \beta_{2c}$, (III) $\beta_{2c} < \beta_1 \leq \beta_{3c}$, and (IV) $\beta_{3c} < \beta_1 < \beta_M$, where $\beta_M = \min\{1+\alpha\mu, 4/3\}$. In the four subintervals of $\beta_1$, we have the following observations. (i) In subinterval I, only negative potential solitary waves can exist and the Mach number $M$ for these waves lies within the interval $M_c < M \leq M_{\max}$, where $M_c$ is the lower bound of $M$ and $M_{\max}$ is the upper bound of $M$, which is defined only when the system can support negative potential solitary waves. (ii) In subinterval II, both negative and positive potential solitary waves can coexist and the Mach number $M$ for these waves lies within the interval $M_c < M < M_D$, whereas only negative potential solitary waves are possible if $M_D < M \leq M_{\max}$. For $M = M_D$ only the positive potential double layer is possible. (iii) In subinterval III, both negative and positive potential solitary waves can coexist and Mach number for these waves lies within $M_c < M \leq M_{\max}$, whereas only positive potential solitary waves are possible if $M_{\max} < M < M_D$ and for $M = M_D$ only positive potential double layer is possible. (iv) In subinterval IV, only positive potential solitary waves can exist and Mach number $M$ for these waves lies within $M_c < M < M_D$; for $M = M_D$ only positive potential double layer solution is possible. A presentation of the four subintervals of $\beta_1$ is shown in Fig. 1.

On the role of dust temperature we have the following observations. $\beta_{1c}$ increases with $\sigma_d$. There exists a value $\sigma_d^*$ of $\sigma_d$ such that $\beta_{2c}$ attains its global minimum value at $\sigma_d = \sigma_d^*$, i.e., $\beta_{2c}$ decreases with increasing $\sigma_d$ for $0 < \sigma_d < \sigma_d^*$ and increases with $\sigma_d$ for $\sigma_d > \sigma_d^*$. For $\beta_{3c}$, we have similar observations. We also observed that for any value of $\sigma_d$ $(0 < \sigma_d < 1)$ we can always find the four subintervals of $\beta_1$ as mentioned earlier. The amplitude of solitary waves decreases with the increase in dust temperature and amplitude of the positive potential double layers decreases with the increase in dust temperature.

Nonthermal ions offer positive potential DAS waves and double layers along with the coexistence of both positive and negative potential solitary waves. In the absence of electron species (i.e., when dust grains are the only source of electrons), which has been observed in different dusty plasma environments,[18,19,30] we have seen that all the four subintervals I, II, III, and IV are well defined and consequently all the results of the DAS waves as presented in this paper hold good.

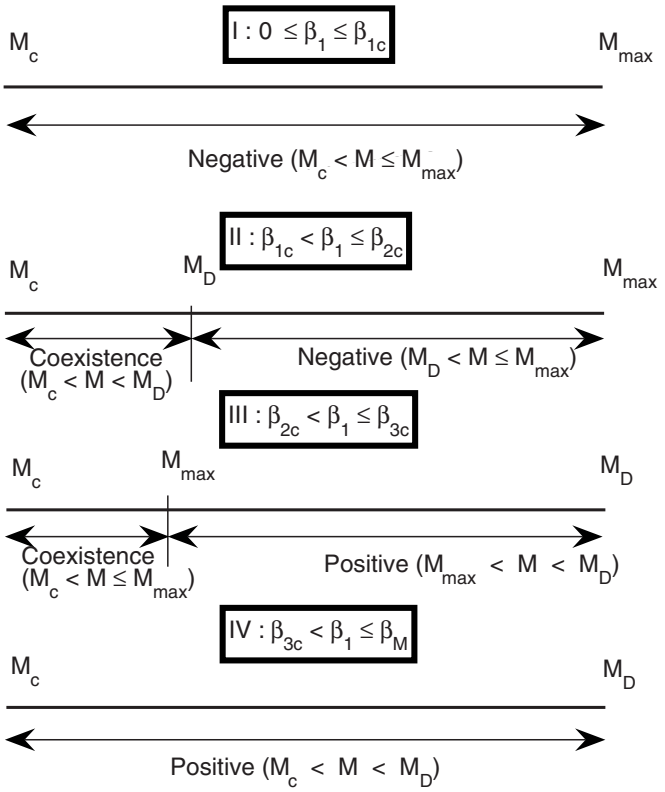


FIG. 1. A graphical presentation of different solitary structures and double layers has been given with respect to four different subintervals of the nonthermal parameter $\beta_1$ within the admissible interval of the Mach number $M$. Here by the words "negative," "coexistence," and "positive" we mean, respectively, existence of negative potential solitary waves, coexistence of both negative and positive potential solitary waves, and existence of positive potential solitary waves. At point $M = M_D$, one can always get a positive potential double layer solution.

Here we express the dust density in such a way that the expression of cold dust particle can be obtained from our result if we put $\sigma_d = 0$ and, consequently, we can compare our result directly with the result of Verheest and Pillay.[16] Comparison of our results with other literatures have also been given.

The present paper is organized as follows. In Sec. II, the basic equations are given. A general theory for existence of different types of solitary waves and double layers has been considered in Sec. III. Numerical and graphical discussions of the different types of solitary waves and double layers have been considered in Sec. IV. Finally, conclusions are given in Sec. V.

## II. BASIC EQUATIONS

The following are the governing equations describing the nonlinear behavior of DA waves, propagating along the $x$-axis, in collisionless dusty plasma consisting of nonthermal ions and isothermal electrons:[20,21]

$$n_{d,t} + (n_d u_d)_x = 0, \tag{1}$$

$$u_{d,t} + u_d u_{d,x} = \phi_x - \sigma_d n_d^{-1} p_{d,x}, \tag{2}$$

$$p_{d,t} + u_d p_{d,x} + \gamma p_d u_{d,x} = 0, \tag{3}$$

$$\phi_{xx} = n_d + \mu_e n_e - \mu_i n_i, \tag{4}$$

where parameters $\sigma_d$, $\mu_e$, and $\mu_i$ are given by the following equation:

$$\sigma_d = \frac{T_d}{Z_d T_i}, \quad \mu_e = \frac{n_{e0}}{Z_d n_{d0}}, \quad \mu_i = \frac{n_{i0}}{Z_d n_{d0}}. \tag{5}$$

Here we used the notation $\psi_{d,q}$ or $(\psi_d)_q$ for $\partial\psi_d/\partial q$ and $n_d$, $n_i$, $n_e$, $u_d$, $p_d$, $\phi$, $x$, and $t$ are, respectively, the dust particle number density, ion number density, electron number density, dust fluid velocity, dust fluid pressure, electrostatic potential, spatial variable, and time, and they have been normalized by $n_{d0}$ (unperturbed dust particle number density), $n_{i0}$ (unperturbed ion number density), $n_{e0}$ (unperturbed electron number density), $c_d(=\sqrt{(Z_d K_B T_i)/m_d})$ (DA speed), $n_{d0}K_B T_d$, $K_B T_i/e$, $\lambda_{Dd}(=\sqrt{(K_B T_i)/(4\pi Z_d n_{d0} e^2)})$(Debye length), and $\omega_{pd}^{-1}(=\sqrt{m_d/(4\pi n_{d0} Z_d^2 e^2)})$ (dusty plasma period). Here $\gamma(=3)$ is the adiabatic index, $K_B$ is the Boltzmann constant, $T_i$, $T_e$, and $T_d$ are, respectively, the average temperatures of ions, electrons, and dust grains, $m_d$ is the mass of a dust particle, $Z_d$ is the number of electrons residing on the dust grain surface, and $e$ is the charge of an electron. Under the above mentioned normalization of the dependent and independent variables, the normalized number density of nonthermal ions can be written following Cairns *et al.*[22] as

$$n_i = (1 + \beta_1\phi + \beta_1\phi^2)e^{-\phi}, \tag{6}$$

where

$$\beta_1 = 4\alpha_1/(1 + 3\alpha_1), \quad \text{with} \quad \alpha_1 \geq 0. \tag{7}$$

It can be easily checked that $0 \leq \beta_1 < 4/3$. Here $\alpha_1$ and consequently $\beta_1$ are parameters that determine the proportion of the fast energetic ions. For isothermal Boltzmann distributed electrons, their normalized number density can be written as

$$n_e = e^{\alpha\phi}, \quad \text{with} \quad \alpha = T_i/T_e. \tag{8}$$

Introducing $\mu = n_{e0}/n_{i0}$, the charge neutrality condition,

$$n_{e0}e + Z_d n_{d0} e - n_{i0} e = 0, \tag{9}$$

can be written as

$$\mu_e = \mu/(1-\mu), \quad \mu_i = 1/(1-\mu). \tag{10}$$

To study the arbitrary amplitude time independent DAS waves and double layers we make all the dependent variables depend only on a single variable $\xi = x - Mt$, where the Mach number $M$ is normalized by $c_d$. Thus, in the steady state, Eqs. (1)–(4) can be written as

$$-Mn_{d,\xi} + (n_d u_d)_\xi = 0, \tag{11}$$

$$-Mu_{d,\xi} + u_d u_{d,\xi} = \phi_\xi - \sigma_d n_d^{-1} p_{d,\xi}, \tag{12}$$

$$-Mp_{d,\xi} + u_d p_{d,\xi} + \gamma p_d u_{d,\xi} = 0, \tag{13}$$

$$\phi_{\xi\xi} = n_d + \mu_e n_e - \mu_i n_i. \tag{14}$$

Using the boundary conditions,

$$\begin{aligned} &n_d \to 1, \quad p_d \to 1, \quad u_d \to 0, \\ &\phi \to 0, \quad \phi_\xi \to 0 \quad \text{as} \quad |\xi| \to \infty, \end{aligned} \tag{15}$$

and solving the Eqs. (11)–(13), we get a quadratic equation for $n_d^2$ and the solution of this quadratic equation of $n_d^2$ can be put in the following form:

$$n_d^2 = \frac{1}{6\sigma_d}(\sqrt{\phi - \Psi_M} - \sqrt{\phi - \Phi_M})^2, \tag{16}$$

where

$$\Psi_M = -\frac{(M - \sqrt{3\sigma_d})^2}{2}, \quad \Phi_M = -\frac{(M + \sqrt{3\sigma_d})^2}{2}. \tag{17}$$

From the expression of $n_d^2$ as given by Eq. (16) we see that $n_d^2$ is non-negative if, and only if, $\sqrt{\phi-\Psi_M}$ and $\sqrt{\phi-\Phi_M}$ are both real. Again $\sqrt{\phi-\Psi_M}$ and $\sqrt{\phi-\Phi_M}$ both are real if and only if $\phi-\Psi_M$ and $\phi-\Phi_M$ are both real and non-negative. However $\phi-\Psi_M$ and $\phi-\Phi_M$ are both real and non-negative if and only if $\phi \geq \Psi_M$ and $\phi \geq \Phi_M$ and finally the conditions $\phi \geq \Psi_M$ and $\phi \geq \Phi_M$ hold simultaneously if and only if $\phi \geq \max\{\Psi_M, \Phi_M\}$. Now from Eq. (17) we see that $\Psi_M \geq \Phi_M (\Leftrightarrow \max\{\Psi_M, \Phi_M\} = \Psi_M)$, consequently Eq. (16) gives theoretically valid expression of $n_d^2$ if and only if $\phi \geq \Psi_M$. However numerically it is not possible to get the correct value of $n_d$ from Eq. (16) for small value of $\sigma_d$ because the denominator of the right hand side of Eq. (16) is $6\sigma_d$. To remove $\sigma_d$ from the denominator of the right hand side of Eq. (16), we first of all note that $(\sqrt{\phi-\Psi_M} + \sqrt{\phi-\Phi_M})^2 > 0$ for all $\phi \geq \Psi_M$ and consequently we can multiply the numerator and the denominator of the right hand side of Eq. (16) by $(\sqrt{\phi-\Psi_M} + \sqrt{\phi-\Phi_M})^2$ and get the following expression of $n_d^2$:

$$n_d^2 = \frac{2M^2}{(\sqrt{\phi - \Psi_M} + \sqrt{\phi - \Phi_M})^2}. \tag{18}$$

With the help of simple algebra Eq. (18) can be written as

$$n_d^2 = \frac{2\left(1 + \dfrac{3\sigma_d}{M^2}\right)^{-1}}{1 + \dfrac{2\phi}{M^2 + 3\sigma_d} + \sqrt{\left(1 + \dfrac{2\phi}{M^2 + 3\sigma_d}\right)^2 - \dfrac{12M^2\sigma_d}{(M^2 + 3\sigma_d)^2}}}. \tag{19}$$

From Eq. (19), we see that this equation gives both theoretically and also numerically correct expression of $n_d^2$ even for any small $\sigma_d \neq 0$, if $\phi \geq \Psi_M$. Now if we put $\sigma_d = 0$ in Eq. (19), we get the same expression of $n_d$ for the cold dust fluid with $\Phi_M = \Psi_M = -(M^2/2)$ as obtained by several authors. However if $\sigma_d = 0$, it is important to note that the dust density undergoes an infinite compression at $\phi = \Psi_M$ and this case has been explicitly investigated by several authors.

Now integrating the Eq. (14) with respect to $\phi$ and using the boundary conditions (15), we get the following equation known as energy integral with $V(\phi)$ as Sagdeev potential or pseudopotential.

$$\frac{1}{2}\left(\frac{d\phi}{d\xi}\right)^2 + V(\phi) = 0, \tag{20}$$

where

$$V(\phi) = V_d + \mu_e V_e - \mu_i V_i, \tag{21}$$

$$V_d = M^2 + \sigma_d - n_d(M^2 + 3\sigma_d + 2\varphi - 2\sigma_d n_d^2), \tag{22}$$

$$V_e = \frac{1}{\alpha}(1 - e^{\alpha\phi}), \tag{23}$$

$$V_i = (1 + 3\beta_1 + 3\beta_1\phi + \beta_1\phi^2)e^{-\phi} - (1 + 3\beta_1). \tag{24}$$

If we put $\sigma_d = \sigma$, $\mu = 0$, $\beta_1 = \beta$, and $\alpha_1 = \alpha$, then it is easy to verify that Eq. (16) of the present paper is equivalent as Eq. (22) of Mendoza-Briceño and co-workers.[19] Similarly if we put $\sigma_d = \sigma$, $\beta_1 = \beta$, $\alpha_1 = \alpha$, and $\alpha = \delta$ and replace $M$ by $M - v_{d0}$ [i.e., if we change the boundary conditions (15) to $n_d \to 1$, $p_d \to 1$, $u_d \to v_{d0}$, $\phi \to 0$, and $\phi_\xi \to 0$ as $|\xi| \to \infty$] then it is easy to verify that Eq. (16) of the present paper is equivalent as Eq. (24) of Maharaj *et al.*[20] and Eq. (26) of Maharaj *et al.*[21]

The energy integral (20) can be regarded as the one-dimensional motion of a particle of unit mass whose position is $\phi$ at time $\xi$ with velocity $d\phi/d\xi$ in a potential well $V(\phi)$. The first term of the energy integral can be regarded as the kinetic energy of the unit mass at position $\phi$ and time $\xi$, whereas $V(\phi)$ is the potential energy at that instant. Since kinetic energy is always a non-negative quantity, $V(\phi) \leq 0$ for the entire motion, i.e., zero is the maximum value for $V(\phi)$. It can be easily checked that $V(0) = V'(0) = 0$, where " $'$ " indicates a derivative with respect to $\phi$. Let us take $V''(0) < 0$, i.e., $\phi = 0$ can be made an unstable position of equilibrium if $V''(0) < 0$ and, consequently, the energy integral can be interpreted as the motion of an oscillatory particle if $V(\phi_m) = 0$ for some $\phi_m \neq 0$, i.e., if the particle is slightly displaced from its unstable position of equilibrium then it moves away from its unstable position of equilibrium and continues its motion until its velocity is equal to zero, i.e., until $\phi$ takes the value $\phi_m$. Now from Eq. (20), we see that $(d^2\phi/d\xi^2) + V'(\phi) = 0$, i.e., the force acting on the particle of unit mass at position $\phi$ at time $\xi$ is $-V'(\phi)$. Therefore, the force acting on the particle of unit mass at position $\phi = \phi_m$ is $-V'(\phi_m)$. For $\phi_m < 0$, the force acting on the particle at the point $\phi = \phi_m$ is directed toward the point $\phi = 0$ if $-V'(\phi_m) > 0$, i.e., if $V'(\phi_m) < 0$. On the other hand, for $\phi_m > 0$, the force acting on the particle at the point $\phi = \phi_m$ is directed toward the point $\phi = 0$ if $-V'(\phi_m) < 0$, i.e., if $V'(\phi_m) > 0$. Therefore, if $V'(\phi_m) > 0$ (for the positive potential side) or if $V'(\phi_m) < 0$ (for the negative potential side) then the particle reflects again to $\phi = 0$. Again, if $V(\phi_m) = V'(\phi_m) = 0$ then the velocity $d\phi/d\xi$ as well as the force $d^2\phi/d\xi^2$ both are equal to zero at $\phi = \phi_m$. Consequently if the particle is slightly displaced from its unstable position of equilibrium ($\phi = 0$) it moves away from $\phi = 0$ and continues its motion until the velocity is equal to zero, i.e., until $\phi$ takes the value $\phi = \phi_m$. However it cannot be reflected again at $\phi = 0$ as the velocity and the force acting on the particle at $\phi = \phi_m$ vanish simultaneously. Actually, if $V'(\phi_m) > 0$ (for $\phi_m > 0$) or if $V'(\phi_m) < 0$ (for $\phi_m < 0$) the particle takes an infinite long time to move away from the unstable position of equilibrium. After that it continues its motion until $\phi$ takes the value $\phi_m$ and again takes an infinite long time to come back its unstable position of equilibrium. Therefore, for the existence of a positive (negative) potential solitary wave solution of the energy integral (20), we must have the following: (a) $V(0) = V'(0) = 0, V''(0) < 0$, (b) $V(\phi_m) = 0, V'(\phi_m) > 0 (V'(\phi_m) < 0)$ for some $\phi_m > 0 (\phi_m < 0)$, and (c) $V(\phi) < 0$ for all $0 < \phi < \phi_m (\phi_m < \phi < 0)$. For the existence of a positive (negative) potential double layer solution of the energy integral (20), we must have the following: (a) $V(0) = V'(0) = 0, V''(0) < 0$, (b) $V(\phi_m) = V'(\phi_m) = 0, V''(\phi_m) < 0$ for some $\phi_m > 0$ $(\phi_m < 0)$, and (c) $V(\phi) < 0$ for all $0 < \phi < \phi_m$ $(\phi_m < \phi < 0)$. Therefore, for the solitary wave solutions of the energy integral (20), (a) is the condition for the position of unstable equilibrium of the particle placed at $\phi = 0$, (b) is the condition for oscillation of the particle within the interval $\min\{0, \phi_m\} < \phi < \max\{0, \phi_m\}$, (c) is the condition to define the energy integral (20) within the interval $\min\{0, \phi_m\} < \phi < \max\{0, \phi_m\}$. For the case of double layers, conditions (a) and (c) remain unchanged but here (b) has been modified in such a way that the particle cannot be reflected again at $\phi = 0$. The mathematical discussion for the existence of solitary wave solutions and double layer solutions of the energy integral (20) have been given in details in Ref. 8 (pp. 105–108).

In the next section we have considered a theoretical discussion of the solitary wave solution and double layer solution of the energy integral (20) with the help of the expression of $V(\phi)$ defined through Eqs. (21)–(24) along with the condition $\phi \geq \Psi_M$, which is necessary as well as sufficient to make $n_d^2$ a non-negative real quantity.

## III. THEORETICAL CONSIDERATION

For the present problem, it can be easily checked that the conditions $V(0) = V'(0) = 0$ are trivially satisfied. From the condition $V''(0) < 0$, we have $M > M_c$, where

$$M_c^2 = 3\sigma_d + \frac{1 - \mu}{1 + \alpha\mu - \beta_1}. \tag{25}$$

From Eq. (25) we find that $M_c^2$ is finite, real, and positive if $\beta_1 < 1 + \alpha\mu$. Therefore, considering the inequalities $0 \leq \beta_1 < 4/3$ and $\beta_1 < 1 + \alpha\mu$, we can conclude that $\beta_1$ is restricted to lie within $0 \leq \beta_1 < \beta_M = \min\{1 + \alpha\mu, 4/3\}$.

To find the upper limit or upper bound of $M$, up to which solitary wave solution can exist, we note from Eqs. (21)–(24) that $V(\phi)$ is real if and only if $n_d$ is real and positive. Again $n_d$ is real and positive if and only if $\phi \geq \Psi_M$. Now we shall consider the following two cases separately.

### A. Negative potential solitary waves and double layers

Consider the existence of negative potential solitary wave for some value of $M$. Therefore, we have

$$V(\phi) < 0 \quad \text{for all} \quad \phi_m < \phi < 0, \qquad V(\phi_m) = 0 \quad , \quad V'(\phi_m) < 0. \tag{26}$$

Now as $V(\phi)$ is real for $\phi \geq \Psi_M$, $\phi_m \geq \Psi_M$ otherwise $V(\phi_m)$ is not a real quantity. Therefore,

$$V(\phi) < 0, \quad \text{for all} \quad \Psi_M (\leq \phi_m) < \phi < 0, \tag{27}$$

defines a large amplitude negative potential solitary wave, which is in conformity with Eq. (26), if $V(\Psi_M)=0$ and $V'(\Psi_M)<0$.

Again let $M_{\max}$ be the maximum value of $M$ up to which solitary wave solution can exist. As $\Psi_M$ decreases with $M$ then $\Psi_{M_{\max}} \leq \Psi_M$. Therefore,

$$V(\phi) < 0, \text{ for all } \Psi_{M_{\max}} (\leq \Psi_M \leq \phi_m) < \phi < 0,$$

defines the largest amplitude solitary waves if $V(\Psi_{M_{\max}})=0$ and $V'(\Psi_{M_{\max}})<0$. It can be easily checked that $V(\Psi_M)$ is a decreasing function of $M$ for $M>M_c$ when the other parameters of the system remain fixed. Also, from the first equation of Eq. (17), we see that $\Psi_M$ is also a decreasing function of $M$ for $M>M_c$. Therefore, $V(\Psi_M)$ is an increasing function of $\Psi_M$ and, consequently, $M_c<M\leq M_{\max} \Rightarrow \Psi_{M_c}>\Psi_M \geq \Psi_{M_{\max}} \Rightarrow V(\Psi_M) \geq V(\Psi_{M_{\max}})=0$. Therefore, for the existence of the negative potential solitary waves, the mach number $M$ is restricted by the following inequality: $M_c<M\leq M_{\max}$, where $M_{\max}$ is the largest positive root of the equation $V(\Psi_M)=0$ and $V(\Psi_M)\geq 0$ for all $M\leq M_{\max}$. Now at $M=M_d$, one can get the negative potential double layer solution if the following conditions hold: (a) $M_d$ is the largest positive root of the equation $V(\Psi_M)=0$, (b) $V'(\Psi_{M_d})=0$, (c) $V''(\Psi_{M_d})<0$, and (d) $V(\phi)<0$ for all $\Psi_{M_d}<\phi<0$.

### B. Positive potential solitary waves and double layers

We have seen earlier that $V(\phi)$ is real if $\phi \geq \Psi_M$, where $\Psi_M$ is strictly negative. For positive potential solitary waves or double layers, we have

$$V(\phi) < 0 \quad \text{for all} \quad 0 < \phi < \phi_m, \tag{28}$$

along with the other conditions stated earlier in this section for positive potential solitary waves or double layers. As $\Psi_M$ is strictly negative and for positive potential solitary waves or double layers, $\phi>0$, the condition $\phi>\Psi_M$ is automatically satisfied and, consequently, for these two cases, $V(\phi)$ is well defined for all $\phi>0$ without imposing extra condition (like $\phi \geq \Psi_M$ as required for the case of negative potential solitary waves or negative potential double layers). For the case of positive potential solitary waves, to find an upper limit or upper bound of $M$, up to which positive potential solitary wave solution can exist, we shall first of all find a value $M_D$ of $M$ for which positive potential double layer solution exists. It can be easily checked numerically that the positive potential double layer solution is the ultimate solution of the energy integral (20) that the present system can encounter, i.e., increasing $M$ beyond $M_D$ no positive potential solitary wave solution can be obtained. It can also be checked that the positive potential double layer solution of the energy integral (20) exists for a particular value of $M(=M_D)$. From this consideration, it is also clear that the positive potential solitary wave solution of the energy integral (20) exists when $M_c<M<M_D$ provided that energy integral (20) gives a double layer solution at $M=M_D$. This is, of course, not a new result because Baboolal *et al.*[34] already reported existence domain for solitons with the help of the existence of a double layer, which may be considered as a limit of a sequence of solitons.

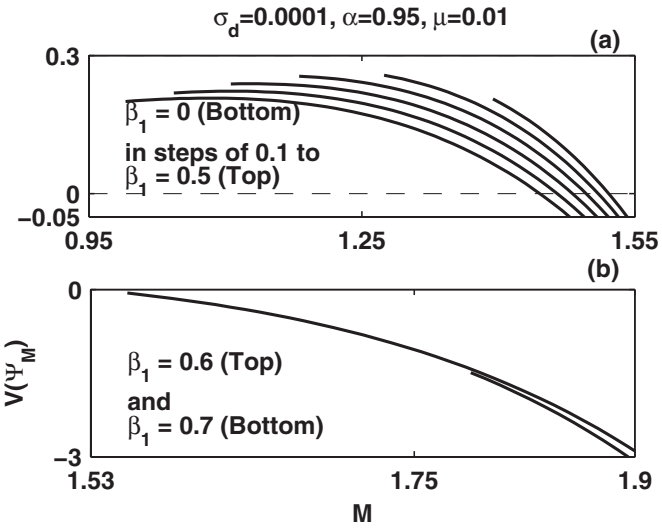


FIG. 2. $V(\Psi_M)$ is plotted against $M$ for different values of $\beta_1$.

## IV. NUMERICAL DISCUSSION

In this section, we have investigated numerically the different types of DAS waves and double layers with the help of a computational scheme. From the expression of $M_c$ as given by Eq. (25), it can be easily checked that $M_c$ increases with $\sigma_d$ for any fixed values of other parameters and $M_c$ increases with $\beta_1$ for any fixed values of other parameters. Further, $M_c$ increases with decreasing $\mu$ for any fixed values of other parameters. It can be verified that $M_c \geq 0.99$ for $\mu=0.01$.

In Fig. 2(a), $V(\Psi_M)$ is plotted against $M$ for different values of $\beta_1$. In this figure each curve starts from the corresponding value of $M_c$. This figure shows how the upper limit ($M_{\max}$) of $M$ changes with $\beta_1$. Here the upper limit ($M_{\max}$), for a particular $\beta_1$, is the $M$-coordinate of the point where the curve intersects the axis of $M$. This figure shows that $M_{\max}$ increases with $\beta_1$. This figure also shows that the length of the interval of $M$, for which negative potential solitary wave solution can exist, decreases with increasing $\beta_1$. In Fig. 2(b), which is a plot of $V(\Psi_M)$ against $M$, no curve crosses the axis of $M$ for $\beta_1>0.6$, i.e., $M_{\max}$ does not exist for $\beta_1>0.6$. So we can conclude that it is impossible to find a negative potential solitary wave for $\beta_1>0.6$.

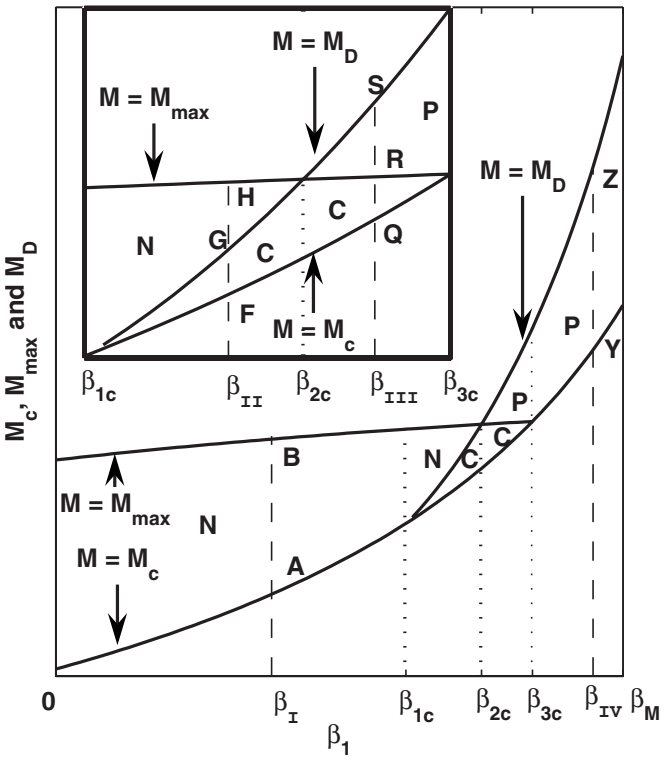


FIG. 3. $M_c$, $M_{\max}$, and $M_D$ have been plotted against $\beta_1$. By "P," "C," and "N" we mean, respectively, the regions for existence of positive potential solitary waves, coexistence of both negative and positive potential solitary waves, and existence of negative potential solitary waves. At any point on the curve $M=M_D$, one can always get a positive potential double layer solution. The region between $\beta_{1c}$ and $\beta_{3c}$ is shown in larger scale in the inset.

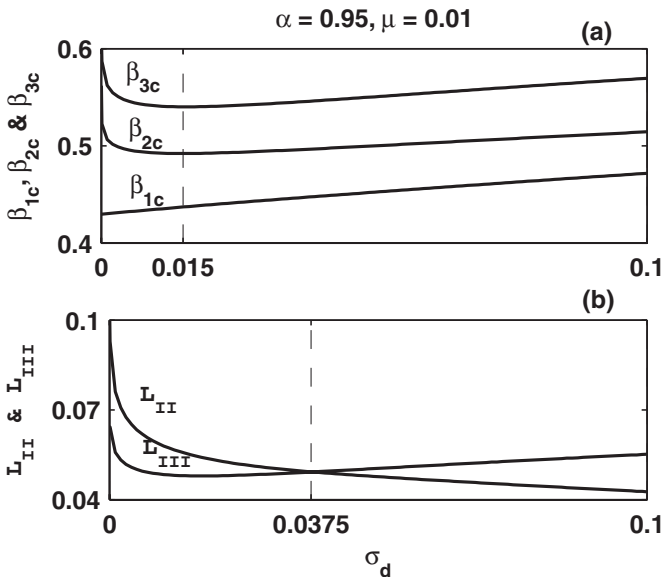


FIG. 4. $\beta_{1c}$, $\beta_{2c}$, and $\beta_{3c}$ are plotted against $\sigma_d$ in (a). In (b), the lengths of intervals II ($L_{II}$) and III ($L_{III}$) are plotted against $\sigma_d$.

For the positive potential solitary wave, there is no such restriction on the upper bound of $M$. However we will see now that the value of $M$ for which double layer solution exists would be the upper bound of $M$.

A computational scheme has been developed by analyzing the Sagdeev potential $V(\phi)$ over the entire interval of $\beta_1: 0 \le \beta_1 < \beta_M$ for fixed values of other parameters $\sigma_d$, $\alpha$, and $\mu$. The results obtained form the numerical computation have been shown graphically in Figs. 3 and 4. In Fig. 3, $M_c$, $M_{\max}$ and $M_D$ have been plotted against $\beta_1$. By "P," "C," and "N" we mean, respectively, the region for existence of positive potential solitary waves, the region for coexistence of both negative and positive potential solitary waves, and the region for existence of negative potential solitary waves. At any point on the curve $M=M_D$, one can always get a positive potential double layer solution. The region between $\beta_{1c}$ and $\beta_{3c}$ is shown in larger scale in the inset. To describe Fig. 3, we used the following notation. By "$M_c(K)$" ("$M_{\max}(K)$") we mean the value of $M_c$ ($M_{\max}$) at point $K$ if $K$ lies on the curve $M=M_c$ ($M=M_{\max}$). Similarly, by "$M_D(K)$" we mean the value of $M_D$ at point $K$ if $K$ lies on the curve $M=M_D$. Now with respect to the four disjoint subintervals, *viz.*, I, II, III, and IV, we have the following four cases only. (i) Consider any point $\beta_I$ of I, i.e., $0 \le \beta_I \le \beta_{1c}$. Let us draw a straight line perpendicular to the $\beta_1$-axis at point $\beta_1=\beta_I$. This straight line intersects the curves $M=M_c$ and $M=M_{\max}$ at points A and B, respectively. Therefore, one can have only negative potential solitary wave solutions if $M_c(A) < M \le M_{\max}(B)$. (ii) Consider any point $\beta_{II}$ of II, i.e., $\beta_{1c} < \beta_{II} \le \beta_{2c}$. Let us draw a straight line perpendicular to the $\beta_1$-axis at point $\beta_1=\beta_{II}$. This straight line intersects the curves $M=M_c$, $M=M_D$, and $M=M_{\max}$ at points $F$, $G$, and $H$, respectively. Then the coexistence of both negative and positive potential solitary waves are possible if $M_c(F) < M < M_D(G)$, whereas for $M_D(G) < M \le M_{\max}(H)$, one can have only negative potential solitary wave solutions and at point $M=M_D(G)$ only positive potential double layer solution is possible. (iii) Consider any point $\beta_{III}$ of III, i.e., $\beta_{2c} < \beta_{III} \le \beta_{3c}$. Let us draw a straight line perpendicular to the $\beta_1$-axis at point $\beta_1=\beta_{III}$. This straight line intersects the curves $M=M_c$, $M=M_{\max}$, and $M=M_D$ at the points $Q$, $R$, and $S$, respectively. Then the coexistence of both negative and positive potential solitary waves are possible if $M_c(Q) < M \le M_{\max}(R)$, whereas for $M_{\max}(R) < M < M_D(S)$, one can have only positive potential solitary wave solutions and at the point $M=M_D(S)$ only positive potential double layer solution is possible. (iv) Consider any point $\beta_{IV}$ of IV, i.e., $\beta_{3c} < \beta_{IV} < \beta_M$. Let us draw a straight line perpendicular to the $\beta_1$-axis at point $\beta_1=\beta_{IV}$. This straight line intersects the curves $M=M_c$ and $M=M_D$ at points $Y$ and $Z$, respectively. Then one can have only positive potential solitary wave solutions if $M_c(Y) < M < M_D(Z)$ and at the point $M=M_D(Z)$ only positive potential double layer solution is possible. It is clear from this figure that negative potential solitary waves exist until $\beta_1$ reaches $\beta_{3c}$, whereas positive potential solitary waves start to exist from $\beta_1=\beta_{1c}$ and, consequently, coexistence of both negative and positive potential solitary waves exist in $\beta_{1c} \le \beta_1 \le \beta_{3c}$. Again, positive potential double layer exists when there is a positive potential solitary wave. In Fig. 4(a), $\beta_{1c}$, $\beta_{2c}$, and $\beta_{3c}$ are plotted against $\sigma_d$. From this figure we see that $\beta_{1c}$ increases with $\sigma_d$. This figure also shows that $\beta_{2c}$ has a global minimum at $\sigma_d=\sigma_d^*$ (say) i.e., $\beta_{2c}$ decreases with increasing $\sigma_d$ for $0 < \sigma_d < \sigma_d^*$ and increases with $\sigma_d$ for $\sigma_d > \sigma_d^*$. For $\beta_{3c}$, we have the similar observations. We have observed that $\sigma_d^*$

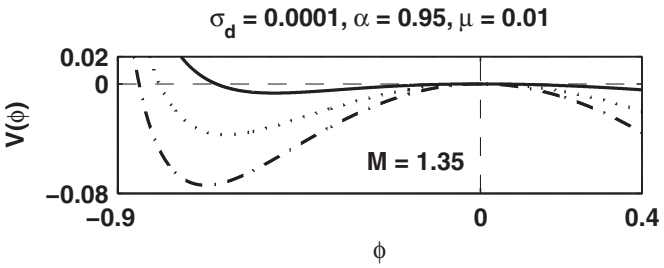


FIG. 5. $V(\phi)$ is plotted against $\phi$ for different values of $\beta_1$. Here the values of $\beta_1$ are 0 [dash-dot $(-\cdot-)$ curve], 0.2 [dotted $(\cdots)$ curve] and 0.4 [solid (—) curve].

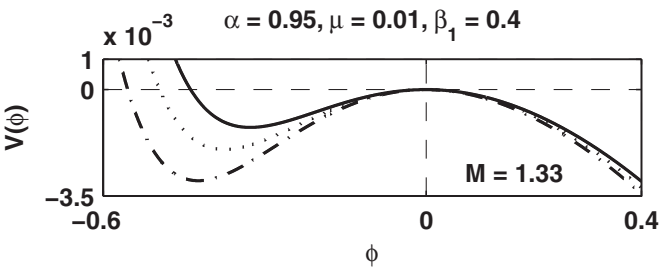


FIG. 7. $V(\phi)$ is plotted against $\phi$ for different values of $\sigma_d$. Here the values of $\sigma_d$ are 0.01 [solid (-) curve], 0.005 [dotted $(\cdots)$ curve] and 0.0001 [dash-dot $(-\cdot-)$ curve].

lies in the neighborhood of $\sigma_d=0.015$ for $\alpha=0.95$ and $\mu=0.01$. Again in Fig. 4(b), we see that the length of the subinterval II ($L_{II}$, say) decreases with increasing $\sigma_d$, whereas the length of the subinterval III ($L_{III}$, say) has a global minimum at $\sigma_d=\sigma_d^{**}$ (say), i.e., $L_{III}$ decreases with increasing $\sigma_d$ for $0<\sigma_d<\sigma_d^{**}$ and increases with $\sigma_d$ for $\sigma_d>\sigma_d^{**}$. We have found that $\sigma_d^{**}$ lies in the neighborhood of $\sigma_d=0.0235$ for $\alpha=0.95$ and $\mu=0.01$. It has also been clear from this figure that at $\sigma_d=\sigma_d^{***}$ (say) the length of the subintervals II and III are equal. We have observed that $\sigma_d^{***}$ lies in the neighborhood of $\sigma_d=0.0375$ for $\alpha=0.95$ and $\mu=0.01$. It is also clear from the Fig. 4(a) that the length of the subinterval I increases with $\sigma_d$, whereas the length of the subinterval IV increases with $\sigma_d$ for $0<\sigma_d<\sigma_d^{*}$ and decreases with increasing $\sigma_d$ for $\sigma_d>\sigma_d^{*}$. Therefore, we can conclude from this figure that the value of $\beta_1$, from which the coexistence of both negative and positive potential solitary waves exist, increases with $\sigma_d$. In this figure we have plotted the curves $\beta_{1c}$, $\beta_{2c}$, and $\beta_{3c}$ as a function of $\sigma_d$ for $0\leq\sigma_d\leq0.1$, to see the behavioral change of $\beta_{1c}$, $\beta_{2c}$, and $\beta_{3c}$, although we have computed numerically the values of $\beta_{1c}$, $\beta_{2c}$, and $\beta_{3c}$ for the entire interval of $\sigma_d$ and we have found that there is no such noticeable change in the behavior of the curves for $\sigma_d>0.1$. We have observed that there is no common point of intersection between any two curves, i.e., for any value of $\sigma_d$, we can always find the four subintervals of $\beta_1$ as mentioned earlier. From our computational scheme, we have found $\beta_{1c}=0.4299$, $\beta_{2c}=0.5229$, and $\beta_{3c}=0.5868$ for $\sigma_d=0.0001$, $\alpha=0.95$, and $\mu=0.01$. In the next few subsections we have shown that all the phenomena, concluded from Fig. 3, are true in nature by means of graphical presentation.

Before going to discuss the different profiles of the solitary waves numerically and graphically, we want to mention the following facts which are helpful to understand the physical situation from the graphical analysis. Let us consider the existence of a positive potential solitary wave with amplitude $\phi_m$. Therefore, we have a point $\phi_{\text{dip}}(0<\phi_{\text{dip}}<\phi_m)$ such that $V(\phi)$ decreases with $\phi$ for $0<\phi<\phi_{\text{dip}}$ (say) and $V(\phi)$ increases for $\phi_{\text{dip}}<\phi<\phi_m$ and at $\phi=\phi_{\text{dip}}$, $V(\phi)$ takes its minimum value. Now the depth of $V(\phi)$=dip of $V(\phi)=|V(\phi_{\text{dip}})|$. Therefore, potential energy takes its minimum value at $\phi=\phi_{\text{dip}}$ and, consequently, the kinetic energy takes its maximum value at $\phi=\phi_{\text{dip}}$. Thus if the dip of $V(\phi)$ [i.e., the depth of $V(\phi)$] increases, the maximum value of kinetic energy increases and, consequently, the amplitude of the solitary wave increases, hence the width decreases. Therefore, the solitary wave becomes more spiky as the depth of the Sagdeev potential increases.

### A. Negative potential solitary waves

In Fig. 5, $V(\phi)$ is plotted against $\phi$ for different values of $\beta_1$ in $0\leq\beta_1\leq0.4$. From Fig. 5, it is clear that for all values of $\beta_1$ in the specified interval only negative potential solitary waves are possible. From this figure it has been observed that the amplitude of the negative potential solitary waves decreases with increasing $\beta_1$. In Fig. 6, the profiles of negative potential solitary waves are plotted against $\xi$ for different $\beta_1$ with $M=1.35$. This figure shows that the amplitude (width) of the negative potential solitary waves decreases (increases) with increasing $\beta_1$. In Fig. 7, $V(\phi)$ is plotted against $\phi$ for different $\sigma_d$. From this figure, we see that the amplitude of the negative potential solitary waves increases with decreasing $\sigma_d$.

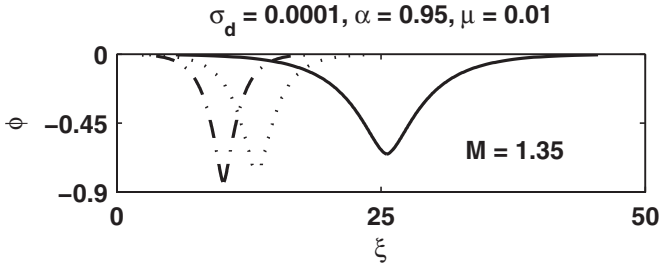


FIG. 6. Profiles of negative potential solitary waves corresponding to Fig. 5.

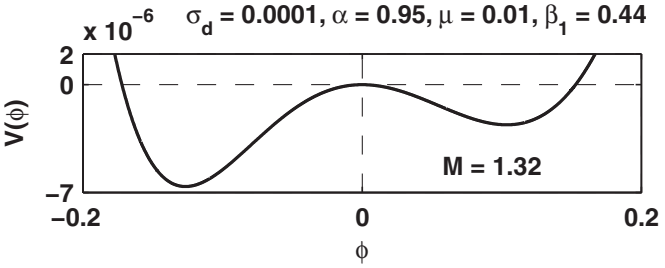


FIG. 8. $V(\phi)$ is plotted against $\phi$. This figure shows the coexistence of both negative and positive potential solitary waves.

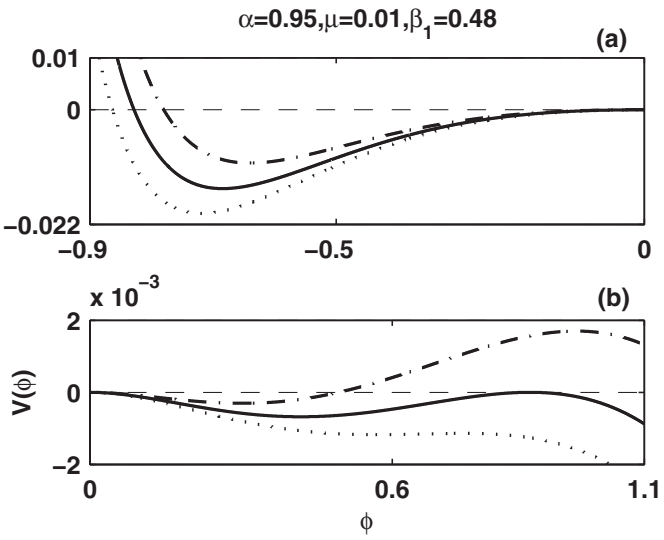


FIG. 9. $V(\phi)$ is plotted against $\phi$ for three different values of $M$. Here $\sigma_d$=0.0001 and the values of $M$ are 1.4 [dash-dot (−·−) curve], 1.42 [dotted (···) curve], and 1.4111 [solid (-) curve]. Negative and positive potential sides have been shown in (a) and (b), respectively. This figure shows that the system can support three different solutions for three different Mach numbers.

### B. Coexistence of both negative and positive potential solitary waves along with positive potential double layers

In Fig. 8, $V(\phi)$ is plotted against $\phi$. This figure shows that both negative and positive potential solitary wave solutions are possible. From this figure we observe that the positive potential side is much flatter than the negative potential side and the amplitude on the negative potential side is larger than that of the positive potential side. In Figs. 9(a) and 9(b), $V(\phi)$ is plotted against $\phi$ for three different values of $M$, which encounter three different solutions. The curve corresponding to $M=1.4$ shows the existence of both the negative and positive potentials (i.e., coexistence) solitary waves, the curve corresponding to $M=1.42$ shows the existence of negative potential solitary wave while the curve corresponding to $M=1.4111$ shows the simultaneous existence of a negative potential solitary wave and a positive potential double layer. From Fig. 9(b), it is clear that the amplitude of the double layer solution is larger than the amplitude of the positive potential solitary waves and the amplitude of the double layer solution is the maximum amplitude on the positive potential side. In Fig. 10, $V(\phi)$ is plotted against $\phi$ for different $\sigma_d$. One can easily verify from this figure that amplitude on both sides increases with decreasing $\sigma_d$ and the amplitude of negative potential solitary wave is greater than that of the positive potential solitary wave. It can also be noticed that for each curve, the positive potential side is much flatter than the negative potential side and consequently the solitary wave profile of the negative potential side becomes more spiky than that of the positive potential side. In Fig. 11, profiles of both negative and positive potential solitary waves are plotted against $\xi$ for two different values of $\beta_1$. This figure shows that the amplitude of both (negative and positive potential) solitary waves decreases with increasing $\beta_1$. In Fig. 12, $V(\phi)$ is plotted against $\phi$ for different values of $\sigma_d$. This figure shows that the dust tem-

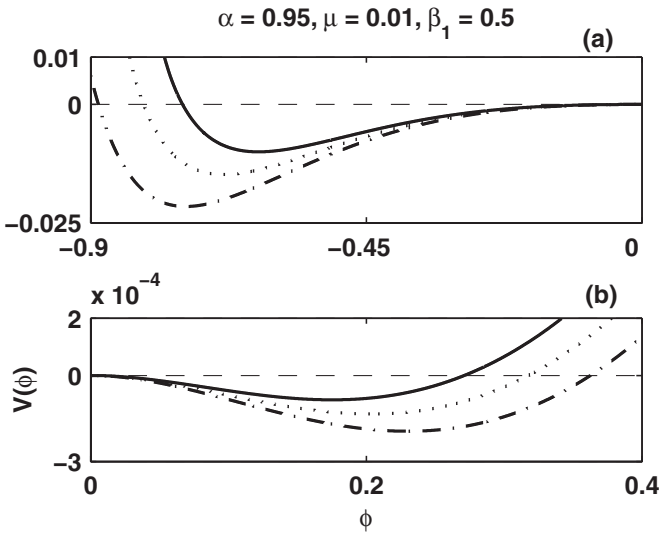


FIG. 10. $V(\phi)$ is plotted against $\phi$ for different values of $\sigma_d$. Here the values of $\sigma_d$ are 0.01 [solid (-) curve], 0.005 [dotted (···) curve], and 0.0001 [dash-dot (−·−) curve]. Negative and positive potential sides have been shown in (a) and in (b), respectively. This figure shows the coexistence of both negative and positive potential solitary waves.

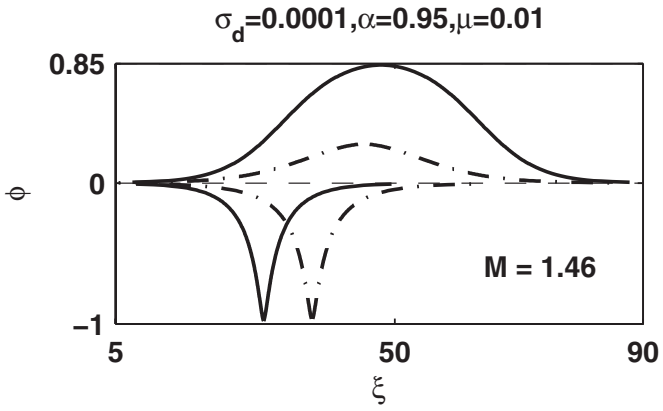


FIG. 11. Profiles of both negative and positive potential solitary waves are plotted against $\xi$ for two different values of $\beta_1$. Here the values of $\beta_1$ are 0.5 [solid (-) curve] and 0.52 [dash-dot (−·−) curve].

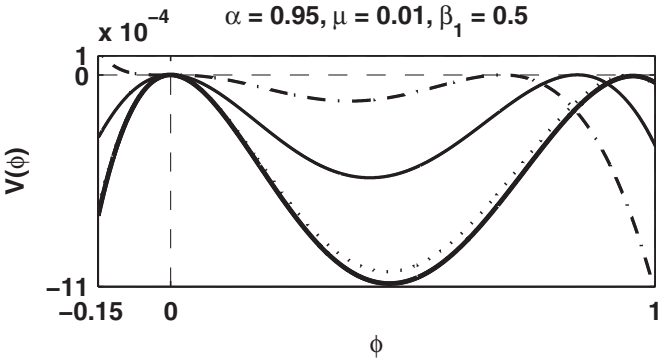


FIG. 12. $V(\phi)$ is plotted against $\phi$ for different values of $\sigma_d$. Here the values of $\sigma_d$ are 0.0001 [bold solid (–) curve], 0.01 [dotted (···) curve], 0.1 [solid (—) curve], and 0.2 [dash-dot (−·−) curve].

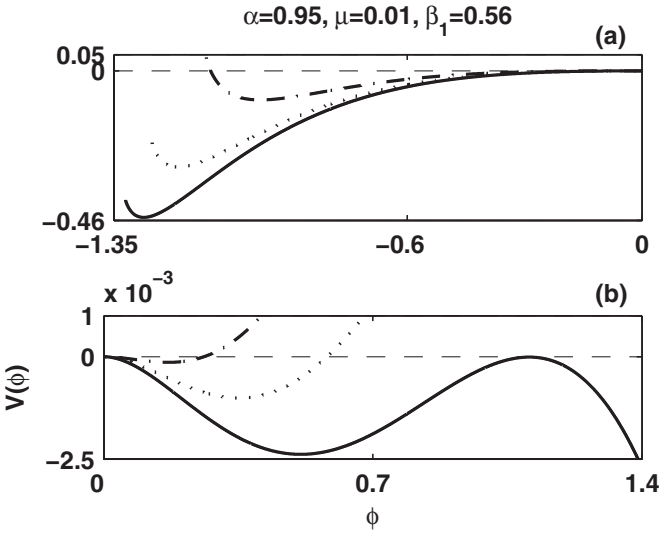


FIG. 13. $V(\phi)$ is plotted against $\phi$ for three different values of $M$ which encounter three different solutions. Here $\sigma_d=0.0001$ and the values of $M$ are 1.5 [dash-dot $(-\cdot-)$ curve], 1.6 [dotted $(\cdots)$ curve], and 1.642 49 [solid (-) curve]. Negative and positive potential sides have been shown in (a) and in (b), respectively.

perature has negligible effect on the amplitude of the positive potential double layer for small $\sigma_d$. However the amplitude of the positive potential double layer decreases with increasing $\sigma_d$.

From Fig. 3, we see that for $\beta_{2c}<\beta_1\leq\beta_{3c}$, there exist three different solitary wave solutions (*viz.*, coexistence, positive potential solitary wave, and positive potential double layer) for different intervals of $M$. This fact is exhibited graphically in Fig. 13. This figure shows that the amplitude of the positive potential double layer is larger than that of the positive potential solitary wave.

### C. Positive potential solitary waves and double layers

From Fig. 3, it is clear that for $\beta_1>\beta_{3c}$, only positive potential solitary waves are possible for $M_c<M<M_D$ and the positive potential solitary waves terminate when the system encounters a positive potential double layer at $M=M_D$. We have represented it graphically in Fig. 14, where $V(\phi)$ is plotted against $\phi$ for two different values of $M$. In this figure we have shown only the positive potential side, whereas it has been observed that on the negative potential side $V(\phi)$ is negative and never crosses the $\phi$-axis. This figure also shows

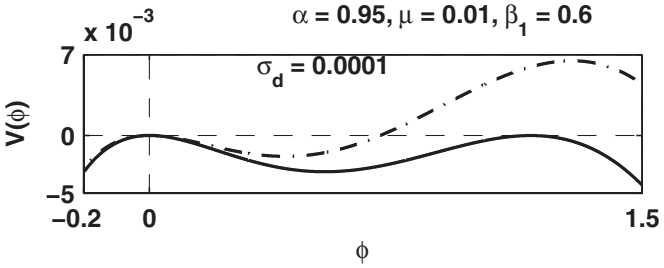


FIG. 14. $V(\phi)$ is plotted against $\phi$ for two different values of $M$ which encounter two different solutions. Here the values of $M$ are 1.75 [dash-dot $(-\cdot-)$ curve] and 1.7935 [solid (-) curve].

that amplitude of the double layer is maximum and this nature remains same for $\beta_1<\beta_M$. It has been observed that for values of $\beta_1>0.6$, the values of $M$, for which positive potential solitary waves are possible, increases much faster than for $\beta_1<0.6$.

We have already mentioned just after Eq. (19) that we can successfully use our model for $\sigma_d=0$. For $\sigma_d=0$, $\alpha=1$, and $\mu=0$, if we apply our computational scheme, we get $\beta_{1c}=0.410\,96$, $\beta_{2c}=0.528\,55$, and $\beta_{3c}=0.614\,55$. These values of $\beta_{1c}$, $\beta_{2c}$, and $\beta_{3c}$ are exactly same as those of Verheest and Pillay.[16] However it is not possible to compare our results with the results of Mendoza-Briceño *et al.*[19] because they used the criteria $(d^3V(0)/d\phi^3)|_{M=M_c}>0$ to find the positive potential solitary waves. However this condition gives incorrect result as extensively pointed out by Verheest and Pillay.[16]

## V. CONCLUSIONS

The properties of arbitrary amplitude DAS waves and double layer in nonthermal plasmas consisting of negatively charged dust grains, nonthermal ions, and isothermal electrons including the effect of dust temperature, are systematically and explicitly investigated with the help of the Sagdeev potential. The results, which have been found from this investigation, can be summarized as follows. Depending on the nature of existence of solitary waves and double layers, the entire interval of $\beta_1$ can be partitioned into four disjoint subintervals: (I) $0\leq\beta_1\leq\beta_{1c}$, (II) $\beta_{1c}<\beta_1\leq\beta_{2c}$, (III) $\beta_{2c}<\beta_1\leq\beta_{3c}$, and (IV) $\beta_{3c}<\beta_1<\beta_M$. For $0\leq\beta_1\leq\beta_{1c}$ $(\beta_{3c}<\beta_1<\beta_M)$, only negative (positive) potential solitary waves are possible if $M_c<M\leq M_{\max}$ $(M_c<M<M_D)$. For $\beta_{1c}<\beta_1\leq\beta_{2c}$ $(\beta_{2c}<\beta_1\leq\beta_{3c})$, both negative potential and positive potential solitary waves are possible if $M_c<M<M_D$ $(M_c<M\leq M_{\max})$, whereas only negative (positive) potential solitary waves are possible if $M_D<M\leq M_{\max}$ $(M_{\max}<M<M_D)$. In all the four cases, only a positive potential double layer solution is possible at $M=M_D$. On the role of dust temperature we have the following observations. $\beta_{1c}$ increases with $\sigma_d$. There exists a value $\sigma_d^*$ of $\sigma_d$ such that $\beta_{2c}$ decreases with increasing $\sigma_d$ for $0<\sigma_d<\sigma_d^*$ and increases with $\sigma_d$ for $\sigma_d>\sigma_d^*$. For $\beta_{3c}$, we have the similar observations. We have observed that for any value of $\sigma_d$ $(0\leq\sigma_d<1)$ we can always find the four subintervals of $\beta_1$. We have also observed that the length of the subintervals II and III are equal for particular value of $\sigma_d$. The amplitude of both solitary waves and double layers decreases with increasing $\sigma_d$.

## ACKNOWLEDGMENTS

The authors are grateful to the referee for his comments for the improvement of this paper. One of the authors (A.D.) is thankful to the State Government Departmental Fellowship Scheme for providing research support.

[1] M. Horanyi and D. A. Mendis, Astrophys. J. **294**, 357 (1985).
[2] M. Horanyi and D. A. Mendis, Astrophys. J. **307**, 800 (1986).
[3] C. K. Goertz, Rev. Geophys. **27**, 271, DOI: 10.1029/RG027i002p00271 (1989).
[4] T. G. Northrop, Phys. Scr. **45**, 475 (1992).

[5]D. A. Mendis and M. Rosenberg, IEEE Trans. Plasma Sci. **20**, 929 (1992).
[6]D. A. Mendis and M. Rosenberg, Annu. Rev. Astron. Astrophys. **32**, 419 (1994).
[7]F. Verheest, Space Sci. Rev. **77**, 267 (1996).
[8]F. Verheest, *Waves in Dusty Space Plasmas* (Kluwer Academic, Dordrecht, 2000).
[9]P. K. Shukla and A. A. Mamun, *Introduction to Dusty Plasma Physics* (IoP, Bristol, 2002).
[10]N. N. Rao, P. K. Shukla, and M. Y. Yu, Planet. Space Sci. **38**, 543 (1990).
[11]A. Barkan, R. L. Merlino, and N. D'Angelo, Phys. Plasmas **2**, 3563 (1995).
[12]G. Praburam and J. Goree, Phys. Plasmas **3**, 1212 (1996).
[13]J. B. Pieper and J. Goree, Phys. Rev. Lett. **77**, 3137 (1996).
[14]H. Washimi and T. Taniuti, Phys. Rev. Lett. **17**, 996 (1966).
[15]R. Z. Sagdeev, in *Reviews of Plasma Physics*, edited by M. A. Leontovich (Consultant Bureau, New York, 1966), Vol. 4.
[16]F. Verheest and S. R. Pillay, Phys. Plasmas **15**, 013703 (2008).
[17]F. Verheest, Phys. Plasmas **16**, 013704 (2009).
[18]A. A. Mamun, R. A. Cairns, and P. K. Shukla, Phys. Plasmas **3**, 2610 (1996).
[19]C. A. Mendoza-Briceño, S. M. Russel, and A. A. Mamun, Planet. Space Sci. **48**, 599 (2000).
[20]S. K. Maharaj, S. R. Pillay, R. Bharuthram, S. V. Singh, and G. S. Lakhina, Phys. Scr. **T113**, 135 (2004).
[21]S. K. Maharaj, S. R. Pillay, R. Bharuthram, R. V. Reddy, S. V. Singh, and G. S. Lakhina, J. Plasma Phys. **72**, 43 (2006).
[22]J. R. Asbridge, S. J. Bame, and I. B. Strong, J. Geophys. Res. **73**, 5777, DOI: 10.1029/JA073i017p05777 (1968).
[23]W. C. Feldman, R. C. Anderson, S. J. Bame, S. P. Gary, J. T. Gosling, D. J. McComas, M. F. Thomsen, G. Paschmann, and M. M. Hoppe, J. Geophys. Res. **88**, 96, DOI: 10.1029/JA088iA01p00096 (1983).
[24]R. Lundin, A. Zakharov, R. Pellinen, H. Borg, B. Hultqvist, N. Pissarenko, E. M. Dubinin, S. W. Barabash, I. Liede, and H. Koskinen, Nature (London) **341**, 609 (1989).
[25]Y. Futaana, S. Machida, Y. Saito, A. Matsuoka, and H. Hayakawa, J. Geophys. Res. **108**, 1025, DOI: 10.1029/2002JA009366 (2003).
[26]R. A. Cairns, A. A. Mamun, R. Bingham, R. Böstrom, R. O. Dendy, C. M. C. Nairn, and P. K. Shukla, Geophys. Res. Lett. **22**, 2709, DOI: 10.1029/95GL02781 (1995).
[27]R. A. Cairns, R. Bingham, R. O. Dendy, C. M. C. Nairn, P. K. Shukla, and A. A. Mamun, J. Phys. IV **5**, C6-43 (1995).
[28]R. A. Cairns, A. A. Mamun, R. Bingham, and P. K. Shukla, Phys. Scr. **T63**, 80 (1996).
[29]A. A. Mamun and R. A. Cairns, J. Plasma Phys. **56**, 175 (1996).
[30]A. A. Mamun, R. A. Cairns, and P. K. Shukla, Phys. Plasmas **3**, 702 (1996).
[31]A. Bandyopadhyay and K. P. Das, J. Plasma Phys. **62**, 255 (1999); **65**, 131 (2001); **68**, 285 (2002); Phys. Scr. **61**, 92 (2000); **63**, 145 (2001); Phys. Plasmas **7**, 3227 (2000); **9**, 465 (2002); **9**, 3333 (2002).
[32]J. Das, A. Bandyopadhyay and K. P. Das, J. Plasma Phys. **72**, 587 (2006); **73**, 869 (2007); **74**, 163 (2008); Phys. Plasmas **14**, 092304 (2007).
[33]Sk. A. Islam, A. Bandyopadhyay, and K. P. Das, J. Plasma Phys. **74**, 765 (2008); Phys. Plasmas **16**, 022307 (2009).
[34]S. Baboolal, R. Bharuthram, and M. A. Hellberg, J. Plasma Phys. **44**, 1 (1990).